Proceeding of the IEEE
International Conference on Robotics and Biomimetics
Dali, China, December 2019

Design and Kinematics Analysis of UPR-UPU-UR Parallel Vector Propulsion Mechanism for Underwater Vehicles

Shuqi Liu
School of Mechanical and Electrical Engineering
Shenzhen Polytechnic
Shenzhen, Guangdong Province, China
mail: 809705010@qq.com

Wei Zhao*
School of Mechanical and Electrical Engineering
Shenzhen Polytechnic
Shenzhen, Guangdong Province, China
mail:zhaowei@szpt.edu.cn

***Abstract* –A two-degree-of-freedom parallel vector propulsion mechanism is proposed, and a suitable coordinate system is established. The position inverse solution, workspace, velocity and acceleration models of UPR-UPU-UR parallel vector propulsion mechanism are constructed by analytical geometry method and closed-loop constraint equation, and the accuracy is verified. Numerical verification was performed using MATLAB to determine the correctness of the theoretical analysis.Finally, the singularity of the mechanism is analyzed by Jacobi, and the reachable workspace of the parallel mechanism is solved by numerical search method. It verifies the rationality of the mechanism motion performance and theoretical analysis.**

Index Terms - Underwater robot; vector propulsion mechanism; kinematic model

I. INTRODUCTION

With the deepening of marine research, people's requirements for the performance of underwater robots are also increasing. Among them, the underwater vector propulsion method has attracted more and more researchers' attention. At present, the vector propulsion mechanism is limited to the series mechanism [1-3]. Although it has good vector propulsion performance, it has many defects such as driving joints, difficulty in control, single motion posture and poor rigidity. The parallel mechanism has the advantages of simple control, rich posture adjustment and high rigidity. It can generate other spatial orientation adjustment movements according to the requirements of the robot movement control task. However, the existing multi-degree-of-freedom parallel mechanism has too many degrees of freedom [4], and it is difficult to apply to vector propulsion of underwater robots in structure. The vector propulsion mechanism UPR-UPU-UR studied in this paper belongs to a new type of vector propulsion method [5-7]. The mechanism has two degrees of rotational freedom, and the working space is large. The propeller is generated by the driving of the branch. The driving force of the deflection enables free deflection of the underwater space. And its positioning accuracy is high, controllable performance is better, more flexible and flexible.

II. UPR-UPU-UR PARALLEL VECTOR PROPULSION MECHANISM

As shown in Figure 1, the UPR-UPU-UR mechanism consists of two platforms and three branches and some motion pairs (U pairs, P pairs, R pairs), all of which are passed through the universal joint and The platform is connected [8]. And the center points of the gimbals below are all in the same plane. The spindle branch UR passes through the rotating pair R through the center of the moving platform, and the branch-UPR is connected to the moving platform by rotating the R pair, and the branch two is connected to the moving platform through the U pair, and the center points of the three moving pairs are also On the same plane, the position of the platform does not change and changes. The branch one and the branch two are two moving pairs, which can be converted into a lead screw (ie, a spiral pair) by a rotating electric machine when actually used. The goal of the design of the mechanism is to use the elongation and shortening of the two deflecting branches 1 and 2 to drive the yaw movement of the moving platform in the space, thereby driving the propeller main shaft to deflect, so as to generate a freely transformable propulsion force, thereby making the underwater The robot performs movements such as steering.

Record that the center point of the universal joint of the UR axis on the platform is O, and the center of the rotating sub-center on the moving platform is P. The center points of the joints of the two yaw-driven branches 1 and the branch 2 connected to the fixed platform are respectively denoted as A1 and A_2, and the center point of the rotation of the branch-and-moving platform is B_1, the branch two and the moving The center point of the joint of the platform is B_2; in addition, the R-axis of the branch one is perpendicular to the spindle branch R and perpendicular to the moving pair P of the branch one; in the joint shaft of the branch two and the movable platform, one axis and the moving platform are in the same In the plane, perpendicular to the central axis of rotation of the spindle, the other axis is perpendicular to the line pair connected to the joint. In addition, it is also required that the positional relationship of the three universal joints on the fixed platform is such that the pair of the spindle joint shaft and the branching joint shaft maintain a vertical relationship, and the other pair maintains a collinear relationship. Therefore, after determining the positional relationship, we establish the coordinate system O-XYZ at point O. As shown in Figure 1, the positive X-axis direction points from point O to point A_2, and the positive direction of the Y-axis points from point A_1 to point O, by Descartes. The right hand rule shows that the positive direction of the Z axis is perpendicular to the fixed platform; the coordinate system P-xyz is established on the moving platform, the positive direction of the x axis points from point P to point B_2, and the positive direction of the y axis points from point B_1 to point P, z The positive direction of the axis is perpendicular to the moving platform. At the same time, the branch

978-1-7281-6321-5/19//$31.00 ©2019 IEEE

coordinate system A_i-$x_iy_iz_i$ is established at the point A_i, where z_i points from point A to point B along the axial direction of the branch rod, and the other two axes follow the axis of the universal joint, which is determined by the right hand rule, and they are also When dynamically changing with the motion of the mechanism, its pose can be expressed according to the rotation matrix. Finally, the length of each component is: $OA_1=OA_2=R$, $PB_1=PB_2=r$, $OP=h$.

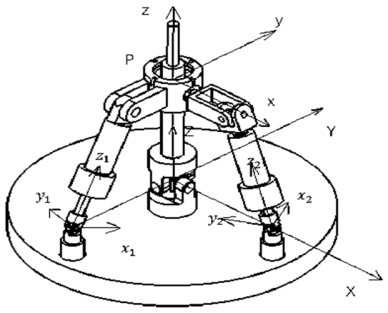

Fig. 1 UPR-UPU-UR parallel mechanism coordinate system diagram

III. KINEMATIC MODELING OF UPR-UPU-UR PARALLEL VECTOR PROPULSION MECHANISM

A. Position Modeling

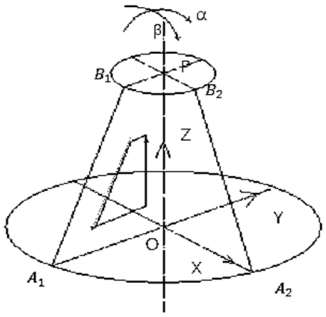

Fig. 2 Schematic diagram of the organization coordinates

This section uses the analytical method to analyze the position inverse of the UPR-UPU-UR parallel mechanism[9-10]. We can calculate from the spiral theory that the parallel mechanism has 2 degrees of freedom, so the orientation change can be expressed by two rotation angles (α and β), and the platform pose can be obtained. As shown in Figure 4, the position vectors of the U sub-center point A_1 of the branch one on the fixed platform and the U sub-center point A_2 of the branch two in the fixed coordinate system {O} are respectively $A_1=[0\ -R\ \ 0]^T$, $A_2=[R\ \ 0\ \ 0]^T$. The position coordinates of the motion center point of the branch one and the branch two on the moving platform in the moving coordinate system{P}are$B_1=[0\ -r\ \ 0]^T$ $B_2=[r\ \ 0\ \ 0]^T$; The rotation angle α of the moving platform (the rotation angle of the moving platform about the X axis) and β (the rotation angle of the moving platform about the Y axis). The rotation matrix of the moving platform relative to the fixed platform base coordinate system can be obtained as follows:

$$ {}^{O}_{P}R = R(X,\alpha)R(Y,\beta) = \begin{pmatrix} c_\beta & 0 & s_\beta \\ s_\alpha s_\beta & c_\alpha & -s_\alpha c_\beta \\ -c_\alpha s_\beta & s_\alpha & c_\alpha c_\beta \end{pmatrix} \tag{1} $$

For convenience of expression, the general robot mechanism specifies that the trigonometric function is written as: $\sin\alpha=s_\alpha$, $\cos\alpha=c_\alpha$, $\sin\beta=s_\beta$, $\cos\beta=s_\beta$, and the shorthand expression is used hereinafter. In the case of the above-mentioned change of the angle of rotation, when the length of the OP is h, the position vector of the origin P of the moving coordinate system {P} fixed on the moving platform in the fixed coordinate system on the fixed platform is:

$$ \vec{P} = {}^{0}_{P}R \cdot \vec{p} = \begin{pmatrix} c_\beta & 0 & s_\beta \\ s_\alpha s_\beta & c_\alpha & -s_\alpha c_\beta \\ -c_\alpha s_\beta & s_\alpha & c_\alpha c_\beta \end{pmatrix} \begin{pmatrix} 0 \\ 0 \\ h \end{pmatrix} = \begin{pmatrix} hs_\beta \\ -hs_\alpha c_\beta \\ hc_\alpha c_\beta \end{pmatrix} \tag{2} $$

Where = [0 0 h] T is the position vector of the origin P of the initial state lower moving coordinate system {P} in a fixed coordinate system.

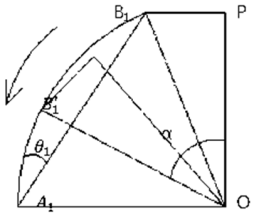

Fig. 3 Branch-one motion quadrilateral constraint

In the fixed coordinate system of the fixed platform, the UPR drive branch, the static platform, the moving platform and the UR main drive shaft are connected end to end to form a quadrilateral structure as shown in Fig. 5, and the dynamic constraint relationship is represented by a vector:

$$ \boldsymbol{l_{OA_1}} + \boldsymbol{l_{A_1B_1}} = \boldsymbol{l_{OP}} + \boldsymbol{l_{PB_1}} \tag{3} $$

Therefore, the closed-loop constraint equation generated by the mechanism under the UPR branch is as shown in equation (10):

$$ \boldsymbol{OA_1} + l_1\boldsymbol{s_1} = \boldsymbol{b_1} \tag{4} $$

among them, $\boldsymbol{OA_1}=[0\ \ -R\ \ 0]^T$ 1 is the position vector in the fixed coordinate system O of the A_1 point on the fixed platform; l_1 is the vector $\boldsymbol{l_{A_1B_1}}$ of the branched one; $\boldsymbol{s_1}$ is the unit vector of the vector $\boldsymbol{l_{A_1B_1}}$ of the branched one in the fixed coordinate system O, that is, the branch one The representation of the axial unit vector in a fixed coordinate system; $\boldsymbol{b_1}$ is the position vector of the B_1 point of the connected moving platform in a fixed coordinate system;

$$ \vec{b}_1 = {}^{0}_{P}R \cdot {}^{P}B_1 + \vec{P} = \begin{pmatrix} c_\beta & 0 & s_\beta \\ s_\alpha s_\beta & c_\alpha & -s_\alpha c_\beta \\ -c_\alpha s_\beta & s_\alpha & c_\alpha c_\beta \end{pmatrix} \begin{pmatrix} 0 \\ -r \\ 0 \end{pmatrix} + \begin{pmatrix} hs_\beta \\ -hs_\alpha c_\beta \\ hc_\alpha c_\beta \end{pmatrix} $$

$$ = \begin{pmatrix} 0 \\ -rc_\alpha \\ -rs_\alpha \end{pmatrix} + \begin{pmatrix} hs_\beta \\ -hs_\alpha c_\beta \\ hc_\alpha c_\beta \end{pmatrix} = \begin{pmatrix} hs_\beta \\ -rc_\alpha - hs_\alpha c_\beta \\ -rs_\alpha + hc_\alpha c_\beta \end{pmatrix} \tag{5} $$

$$ \boldsymbol{l_1 s_1} = \boldsymbol{b_1} - \boldsymbol{OA_1} = \begin{pmatrix} hs_\beta \\ -rc_\alpha - hs_\alpha c_\beta \\ -rs_\alpha + hc_\alpha c_\beta \end{pmatrix} - \begin{pmatrix} 0 \\ -R \\ 0 \end{pmatrix} = \begin{pmatrix} hs_\beta \\ -rc_\alpha - hs_\alpha c_\beta + R \\ -rs_\alpha + hc_\alpha c_\beta \end{pmatrix} \tag{6} $$

From equation (6), the relationship between the unit vector $\boldsymbol{s_1}$ of the driving branch and the rotational angles α and β of the moving platform can be derived as follows:

$$\vec{s}_1 = \frac{b_1 - OA_1}{l_1} = \frac{1}{l_1}\begin{pmatrix} hs_\beta \\ -rc_\alpha - hs_\alpha c_\beta + R \\ -rs_\alpha + hc_\alpha c_\beta \end{pmatrix} \quad (7)$$

According to the attitude angles θ_1 and φ_1 of the UPR branch in the base coordinate system (θ_1 is the rotation angle of the branch 1 around the X axis, and φ_1 is the rotation angle of the branch 1 around the Y axis), the UPR drive branch can be obtained relative to the base coordinate system. The rotation matrix is:

$$^{O}_{A_1}R = R(x,\theta_1)R(y,\varphi_1) = \begin{pmatrix} \vec{x} & \vec{y} & \vec{z} \end{pmatrix} = \begin{pmatrix} c_{\varphi_1} & 0 & s_{\varphi_1} \\ s_{\theta_1}s_{\varphi_1} & c_{\theta_1} & -s_{\theta_1}c_{\varphi_1} \\ -c_{\theta_1}s_{\varphi_1} & s_{\theta_1} & c_{\theta_1}c_{\varphi_1} \end{pmatrix} \quad (8)$$

The unit vector of vector $\boldsymbol{l_{A_1B_1}}$ is expressed in the supporting coordinate system {A1} as: $^1s_1=[0 \quad 0 \quad 1]^T$; then the vector$\boldsymbol{l_{A_1B_1}}$The representation of the unit vector under the fixed coordinate system {O} can also be:

$$\boldsymbol{s_1} = \boldsymbol{^{O}_{A_1}R} \cdot {}^1s_1 = \begin{bmatrix} s_{\varphi_1} & -s_{\theta_1}c_{\varphi_1} & c_{\theta_1}c_{\varphi_1} \end{bmatrix}^T \quad (9)$$

In summary,

$$l_1=\sqrt{h^2s_\beta{}^2 + (-rc_\alpha - hs_\alpha c_\beta + R)^2 + (-rs_\alpha + hc_\alpha c_\beta)^2}$$

$$l_1=\sqrt{r^2 + h^2 + R^2 - 2Rrc_\alpha - 2Rhs_\alpha c_\beta} \quad (10)$$

The relationship between the attitude angles θ_1 and φ_1 of the UPR branch and the rotational angles α and β of the moving platform can be obtained by combining equations (9) and (10).

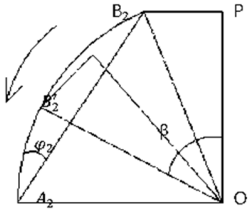

Fig.4 Branched two motion quadrilateral constraints

In the fixed coordinate system of the fixed platform, the UPU drive branch, the fixed platform, the UR main drive shaft and the moving platform form a quadrilateral structure as shown in fig.4, which is similar to the quadrilateral restraint structure formed by the UPR branch. By branch 1 is the same: then the representation of the unit vector of the vector$\boldsymbol{l_{A_2B_2}}$under the fixed coordinate system {O} can also be:

$$\boldsymbol{s_2} = \boldsymbol{^{O}_{A_2}R} \cdot {}^2\boldsymbol{s_2} = \begin{bmatrix} s_{\varphi_2} & -s_{\theta_2}c_{\varphi_2} & c_{\theta_2}c_{\varphi_2} \end{bmatrix}^T \quad (11)$$

$$l_2 = \sqrt{(rc_\beta + hs_\beta - R)^2 + (rs_\alpha s_\beta - hs_\alpha c_\beta)^2 + (-rc_\alpha s_\beta + hc_\alpha c_\beta)^2} \quad (12)$$

Like the UPR branch, the relationship between the attitude angles θ_2 and φ_2 of the UPU branches and the attitude angles α and β of the moving platform can be obtained from the equations(9),(11), and (12).

Finally, the helical pairs of the two yaw-driven branches (as the moving pair analysis) are analyzed as a pair of pistons: the center of mass of the branched piston rod is C_i, the center of mass of the cylinder is D_i, and the distance from C_i to A_i is h_1 The distance from D_i to B_i is h_2, the vector of the fixed coordinate system origin O to C_i is represented as $\boldsymbol{c_i}$, and the vector to D_i is represented as $\boldsymbol{d_i}$ (where i=1, 2), as shown in Figure 2.7. Then the position vector equations of the piston rod and the cylinder centroid of the two drive branches of the parallel mechanism are as follows:

$$\boldsymbol{c_i} = \mathrm{O}\boldsymbol{A_i} + h_1\boldsymbol{s_i} \quad (13)$$

$$\boldsymbol{d_i} = \mathrm{O}\boldsymbol{A_i} + (l_i - h_2)\boldsymbol{s_i} \quad (14)$$

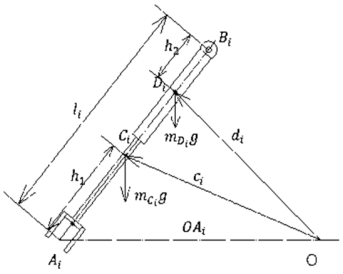

Fig. 5 Branched centroid position

B. Speed Modeling

It is assumed that the attitude angles α and β of the center point P of the moving platform are the same as defined above; the angular velocity vector of the moving platform is set to ω, then the speed of the B_i point at the upper end of the two driving branches connected to the moving platform can be obtained from the foregoing the equation (4) derived on the right side of the equal sign, namely:

$$\boldsymbol{v_{B_i}} = \boldsymbol{\omega} \times \boldsymbol{b_i} \quad (15)$$

Converting$\boldsymbol{v_{B_i}}$ to the branch coordinate system of the drive branch can be expressed as:

$$^i\boldsymbol{v_{B_i}} = \boldsymbol{^{A_i}_{O}R} \cdot \boldsymbol{v_{B_i}} \quad (16)$$

Where $\boldsymbol{^{A_i}_{O}R}$ is the rotation matrix of the branch coordinates relative to the top coordinate system, according to the orthogonality of the coordinate rotation matrix,

$$\boldsymbol{^{A_i}_{O}R} = \boldsymbol{^{O}_{A_i}R^T} \quad (17)$$

It is also possible to derive the time t from the left side of the equation (4) and pass the coordinate transformation between the branch and the base coordinate system to obtain the velocity vector equation in the branch i:

$$^i\boldsymbol{v_{B_i}} = \dot{l_i}\ {}^i\boldsymbol{s_i} + l_i\ {}^i\boldsymbol{\omega_i} \times {}^i\boldsymbol{s_i} \quad (18)$$

Projecting the resulting velocity vector along the direction of the drive rod, ie $\boldsymbol{z_i}$:

$$\dot{l_i} = {}^iv_{B_{i,z}} \quad (19)$$

among them: $\dot{l_i} = \frac{Rr\dot{\alpha}\sin\alpha - Rh\dot{\alpha}\cos\alpha\cos\beta + Rh\dot{\beta}\sin\alpha\sin\beta}{\sqrt{r^2+h^2+R^2-2Rr\cos\alpha-2Rh\sin\alpha\cos\beta}}$

$$\dot{l_2} = \frac{Rr\dot{\beta}\sin\beta - Rh\dot{\beta}\cos\beta}{\sqrt{\boldsymbol{r^2+h^2+R^2-2Rr\cos\beta-2Rh\sin\beta}}}$$

It is precisely because the $\boldsymbol{z_i}$ axis of the supporting coordinate system of the branch is along the direction of the branch rod, the velocity component of $^i\boldsymbol{v_{B_i}}$ in the $\boldsymbol{z_i}$ axis is the relative of the branched piston rod. The linear velocity$\dot{l_i}$ of the branch cylinder.

The angular velocity vector of the driving branch i can be crossed by $^i\boldsymbol{s_i}$ to multiply both ends of (17) to obtain:

$$^i\omega_i = \frac{^iS_i \times {}^iV_{B_i}}{l_i} = \frac{1}{l_i}\begin{pmatrix} {}^iV_{B_{i,y}} \\ {}^iV_{B_{i,x}} \\ 0 \end{pmatrix} \quad (20)$$

In addition, regarding the centroid velocity of the two drive chain cylinders and the piston rod relative to the respective branch coordinate system:

$$ {}^{i}V_{C_i} = h_1 {}^{i}\omega_i \times {}^{i}s_i = \frac{h_1}{l_i}\begin{pmatrix} {}^{i}V_{B_{i,x}} \\ {}^{i}V_{B_{i,y}} \\ 0 \end{pmatrix} \quad (21) $$

$$ {}^{i}V_{D_i} = (l_i - h_2) {}^{i}\omega_i \times {}^{i}s_i + \dot{l}_i \cdot {}^{i}s_i = \frac{1}{l_i}\begin{pmatrix} (l_i - h_2) {}^{i}V_{B_{i,x}} \\ (l_i - h_2) {}^{i}V_{B_{i,y}} \\ l_i \cdot {}^{i}V_{B_{i,z}} \end{pmatrix} \quad (22) $$

C. Acceleration Modeling

The acceleration of the B_i point of the two driving branches connected to the moving platform can be expressed as:

$$ \dot{\boldsymbol{v}}_{\boldsymbol{B_i}} = \dot{\boldsymbol{\omega}} \times \boldsymbol{b_i} + \omega \times (\omega \times \boldsymbol{b_i}) \quad (23) $$

Converting the acceleration $\dot{\boldsymbol{v}}_{\boldsymbol{B_i}}$ to the coordinate system {Ai} of the drive branch can be expressed as:

$$ {}^{i}\dot{\boldsymbol{v}}_{\boldsymbol{B_i}} = {}^{A_i}_{O}\boldsymbol{R} \cdot \dot{\boldsymbol{v}}_{\boldsymbol{B_i}} \quad (24) $$

An expression that drives the acceleration of the branches in their respective chain coordinate systems:

$$ {}^{i}\dot{\boldsymbol{v}}_{\boldsymbol{B_i}} = \ddot{\boldsymbol{l}}_{\boldsymbol{i}} {}^{i}\boldsymbol{s_i} + 2\dot{l}_i({}^{i}\boldsymbol{\omega_i} \times {}^{i}\boldsymbol{s_i}) + l_i {}^{i}\dot{\boldsymbol{\omega}}_{\boldsymbol{i}} \times {}^{i}\boldsymbol{s_i} + l_i {}^{i}\boldsymbol{\omega_i} \times ({}^{i}\boldsymbol{\omega_i} \times {}^{i}\boldsymbol{s_i}) \quad (25) $$

Use ${}^{i}\boldsymbol{s_i}$ point multiplication (24) at both ends to get:

$$ {}^{i}\dot{\boldsymbol{v}}_{\boldsymbol{B_{i,z}}} = \ddot{\boldsymbol{l}}_{\boldsymbol{i}} - l_i {}^{i}\boldsymbol{\omega_i}^2 $$

$$ \ddot{\boldsymbol{l}}_{\boldsymbol{i}} = {}^{i}\dot{\boldsymbol{v}}_{\boldsymbol{B_{i,z}}} + l_i {}^{i}\boldsymbol{\omega_i}^2 = {}^{i}\dot{\boldsymbol{v}}_{\boldsymbol{B_{i,z}}} + \frac{({}^{i}\dot{\boldsymbol{v}}_{\boldsymbol{B_{i,x}}}^2 + {}^{i}\dot{\boldsymbol{v}}_{\boldsymbol{B_{i,y}}}^2)}{l_i} \quad (26) $$

When deflected by the moving sub-drive mechanism, there is ${}^{i}\dot{\boldsymbol{\omega}}_{\boldsymbol{i,z}} = 0$; with ${}^{i}\boldsymbol{s_i}$ cross-multiplier (24):

$$ {}^{i}s_i \times {}^{i}v_{B_i} = l_i {}^{i}\dot{\omega}_i + 2\dot{l}_i {}^{i}\omega_i \quad (27) $$

$$ {}^{i}\dot{\omega}_i = \frac{1}{l_i} {}^{i}s_i \times {}^{i}v_{B_i} - \frac{2\dot{l}_i}{l_i} {}^{i}\omega_i $$

$$ = \frac{1}{l_i^2}\begin{pmatrix} l_i {}^{i}V_{B_{i,y}} \\ -l_i {}^{i}V_{B_{i,x}} \\ 0 \end{pmatrix} - \frac{1}{l_i^2}\begin{pmatrix} 2l_i {}^{i}V_{B_{i,z}} {}^{i}V_{B_{i,y}} \\ -2l_i {}^{i}V_{B_{i,z}} {}^{i}V_{B_{i,x}} \\ 0 \end{pmatrix} = \frac{1}{l_i^2}\begin{pmatrix} l_i {}^{i}V_{B_{i,y}} - 2l_i {}^{i}V_{B_{i,z}} {}^{i}V_{B_{i,y}} \\ -l_i {}^{i}V_{B_{i,x}} + 2l_i {}^{i}V_{B_{i,z}} {}^{i}V_{B_{i,x}} \\ 0 \end{pmatrix} \quad (28) $$

In addition, the acceleration of the two branches of the cylinder and the piston rod at the centroid of the branch coordinates can be obtained by transforming the matrix (20) and (21) by the rotation matrix and deriving:

$$ {}^{i}\dot{v}_{C_i} = h_1 {}^{i}\dot{\omega}_i \times {}^{i}s_i + h_1 {}^{i}\omega_i \times ({}^{i}\omega_i \times {}^{i}s_i) = \frac{h_1}{l_i^2}\begin{pmatrix} l_i {}^{i}\dot{v}_{B_{i,x}} - 2{}^{i}V_{B_{i,z}} {}^{i}V_{B_{i,x}} \\ l_{i_y} {}^{i}\dot{v}_{B_{i_y}} - 2{}^{i}V_{B_{i_y}} {}^{i}V_{B_{i_y}} \\ -({}^{i}V_{B_{i,x}}^2 + {}^{i}V_{B_{i,y}}^2) \end{pmatrix} \quad (29) $$

$$ {}^{i}\dot{v}_{D_i} = 2\dot{l}_i({}^{i}\omega_i \times {}^{i}s_i) + (l_i - h_2) {}^{i}\dot{\omega}_i \times {}^{i}s_i + (l_i - h_2) {}^{i}\omega_i \times ({}^{i}\omega_i \times {}^{i}s_i) + \ddot{l}_i {}^{i}s_i $$

$$ = \frac{1}{l_i}\begin{pmatrix} 2{}^{i}V_{B_{i,z}} {}^{i}V_{B_{i,x}} \\ 2{}^{i}V_{B_{i,z}} {}^{i}V_{B_{i,y}} \\ 0 \end{pmatrix} + \frac{l_i - h_2}{l_i^2}\begin{pmatrix} l_i {}^{i}\dot{v}_{B_{i,x}} - 2{}^{i}V_{B_{i,z}} {}^{i}V_{B_{i,x}} \\ l_i {}^{i}\dot{v}_{B_{i,y}} - 2{}^{i}V_{B_{i,z}} {}^{i}V_{B_{i,y}} \\ 0 \end{pmatrix} $$

$$ +(l_i - h_2)\begin{pmatrix} 0 \\ 0 \\ -({}^{i}V_{B_{i,x}}^2 + {}^{i}V_{B_{i,y}}^2)/l_i^2 \end{pmatrix} + \begin{pmatrix} {}^{i}\dot{v}_{B_{i,z}} + ({}^{i}V_{B_{i,x}}^2 + {}^{i}V_{B_{i,y}}^2)/l_i \end{pmatrix}\begin{pmatrix} 0 \\ 0 \\ 1 \end{pmatrix} $$

$$ {}^{i}\dot{v}_{D_i} = \frac{1}{l_i^2}\begin{pmatrix} l_i(l_i - h_2) {}^{i}\dot{v}_{B_{i,x}} + 2h_2 {}^{i}V_{B_{i,z}} {}^{i}V_{B_{i,x}} \\ l_i(l_i - h_2) {}^{i}\dot{v}_{B_{i,y}} + 2h_2 {}^{i}V_{B_{i,z}} {}^{i}V_{B_{i,y}} \\ h_2({}^{i}V_{B_{i,x}}^2 + {}^{i}V_{B_{i,y}}^2) + l_i^2 {}^{i}\dot{v}_{B_{i,z}} \end{pmatrix} \quad (30) $$

IV. SIMULATION OF UPR-UPU-UR PARALLEL VECTOR PROPULSION MECHANISM

According to the position inverse solution expression obtained in the foregoing, the position output from the known moving platform can be used to find the inverse solution of the position of the mechanism. The algorithm can be implemented by means of matlab software. Assume that the distance between the central axis universal joint center point O of the central axis and the branch universal joint center point A_i is 73.7 mm, and the center point P on the moving platform to the branch R pair (or U pair) center point B_i The distance h = 50 mm, the distance h between the central axis U sub-center point O and the R sub-center point P is 70.0 mm. The attitude parameter outputted by the setting platform in the fixed reference frame is θ=[0.15,0.1] ^{T}, which is brought into the equations (5) and (12) obtained in the foregoing, and the two deflection driving branches in this state are obtained. The lengths are:

$$ l_1 = 66.9, l_2 = 65.4 $$

Then the positional positive solution analysis of the example is carried out, and the above two rod lengths $l = [l_1, l_2]^T$ are taken as the input parameters of the positive position solution, and the pose parameter of the moving platform is solved as θ=[0.15, 0.1] ^{T}, the result is unique, and is the same as the hypothesis output when the position inverse solution is calculated. The reverse verification proves that the positional forward and inverse solution of the parallel mechanism can be solved by the inverse solution expressions (5) and (12).

The following is a parametric simulation of the position inverse solution in matlab: Let the motion time t be 10 s and represent it as a vector of 0 to 10 (pitch 0.1), where a and b represent α and β, respectively. The angular velocities around the X and Y axes are both set to 1°/sec. By measuring, the distance from B_i to the P point of the center of the moving platform in the three-dimensional model is r=50mm, and the distance between the U-sub-center A_i point of the two driving branches UPR and UPU and the origin O of the stationary

platform coordinate system is R=73.7mm. The distance from the center of the moving platform to the origin O of the fixed coordinate system is h=70mm. The expression of the length of the two driving branches L with time t from the expression of the l_i mode of the inverse position solution is shown in Fig. 6. At the same time, the curve of the movement speed of the two chain rods can be obtained as shown in Fig. 7.

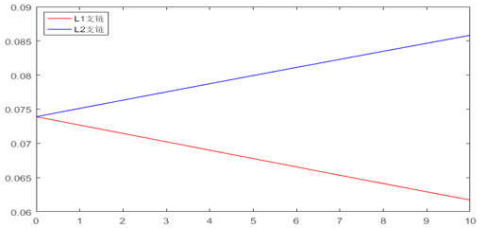

Fig. 6 Curve of the length of two drive branches in matlab with time

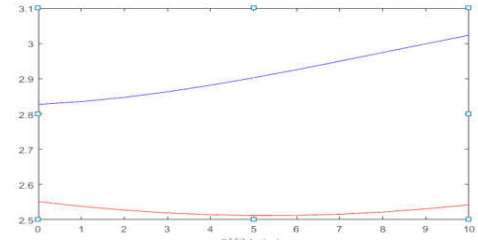

Fig. 7 Curve of the moving speed of two chain rods with time in matlab simulation

V. ANALYSIS OF THE MOTION PERFORMANCE OF UPR-UPU-UR PARALLEL MECHANISM

A. Speed of Jacobi

The length l_i of the two drive chains obtained from the above is a function of the rotational angle of the moving platform about the X-axis or the Y-axis, and $\boldsymbol{\theta}$ is again a function of time t, namely: $\boldsymbol{\theta} = \boldsymbol{g}(\boldsymbol{t})$. According to the meaning of the Jacobian matrix, the Jacobian matrix is calculated by the differential method, and the two equations (5) and (12) of the inverse solution of the above position are derived (for time t):

$$\dot{l}_1 = \begin{bmatrix} a_{11}, a_{12} \end{bmatrix} \begin{pmatrix} \dot{\alpha} \\ \dot{\beta} \end{pmatrix} \tag{31}$$

$$\dot{l}_2 = \begin{bmatrix} a_{21}, a_{22} \end{bmatrix} \begin{pmatrix} \dot{\alpha} \\ \dot{\beta} \end{pmatrix} \tag{32}$$

Where $\dot{\boldsymbol{\theta}}$ (ie $\dot{\alpha}$ and $\dot{\beta}$) represents the angular velocity at which the mechanical platform of the mechanism is deflected about two axes;among them:

$$a_{11} = \frac{R(r\sin\alpha - h\cos\alpha\cos\beta)}{l_1} \tag{33}$$

$$a_{12} = \frac{Rh\sin\alpha\sin\beta}{l_1}, \quad a_{21} = 0 \tag{34}$$

$$a_{22} = \frac{R(r\sin\beta - h\cos\beta)}{l_2} \tag{35}$$

From this, the speed equation of the mechanism is as follows:

$$\begin{bmatrix} \dot{l}_1 \\ \dot{l}_2 \end{bmatrix} = \begin{pmatrix} a_{11} & a_{12} \\ a_{21} & a_{22} \end{pmatrix} \begin{bmatrix} \dot{\alpha} \\ \dot{\beta} \end{bmatrix} \tag{36}$$

It can be seen that, $J = \begin{pmatrix} a_{11} & a_{12} \\ a_{21} & a_{22} \end{pmatrix}$ (37)

Then J is the Jacobian matrix of the parallel propulsion mechanism.

B.Singular Configuration

The previous section has given the speed Jacobi, which can be used to determine whether the singular configuration exists and when there will be singular configurations. The singular configuration is a specific form produced when the mechanism enters a certain critical point. At this time, the degree of freedom of the mechanism is no longer the theoretical value. Therefore, it is necessary to analyze the singularity of the organization to avoid singularity .

Directly making the Jacobian matrix of the mechanism equal to 0, that is, let det(J)=0, then the relationship between the singular configuration and its pose can be solved. The Grassman line geometry method judges the singularity of the mechanism based on the linear relationship between the motion sub-line vectors. In this section, the algebraic method, ie matrix analysis method, is used to calculate the singular configuration of the mechanism described in this paper from the perspective of the speed Jacobian and the mechanism characteristics obtained in the previous paper.

According to the nature of J, the singular configuration of the UPR-UPU-UR parallel mechanism is analyzed by the Jacobian matrix of equation (37) as follows:

$$|J| = \begin{vmatrix} a_{11}, a_{12} \\ a_{21}, a_{22} \end{vmatrix} = \begin{vmatrix} \frac{R(r\sin\alpha - h\cos\alpha\cos\beta)}{l_1}, & \frac{Rh\sin\alpha\sin\beta}{l_1} \\ 0, & \frac{R(r\sin\beta - h\cos\beta)}{l_2} \end{vmatrix} = 0 \tag{38}$$

Finished up:

$$\frac{R(r\sin\alpha - h\cos\alpha\cos\beta)}{l_1} \bullet \frac{R(r\sin\beta - h\cos\beta)}{l_2} = 0 \tag{39}$$

In the formula, since the rod length cannot be zero, $l_1 \neq 0$, $l_2 \neq 0$, and R, r, h are constant values; therefore, the equation is solved:

$$(r\sin\alpha - h\cos\alpha\cos\beta)\cdot(r\sin\beta - h\cos\beta) = 0 \tag{40}$$

The condition values for α and β when the polynomial is equal to 0 can be derived:

$$\beta = \arctan(h/r) \tag{41}$$

$$\alpha = \arctan(h/\sqrt{r^2 + h^2}) \tag{42}$$

Therefore, the mechanism should have a irregular configuration. A simulation of the singular configuration that may occur is shown in Figures 8:

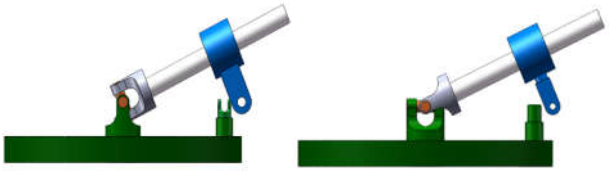

(a) side view (b) front view

Fig. 8 UPR-UPU-UR parallel mechanism singular configuration

In summary, we can see that there will be singular configurations in this mechanism. It is necessary to consider this in the process of motion control to avoid uncontrollable conditions and affect the performance of the organization.

C. Workspace Analysis

The working space of the organization refers to the area that can be reached at the end of the mechanism (that is, the moving platform or the propeller to which it is connected). The UPR-UPU-UR mechanism is used to calculate the reachable workspace by numerical search method to verify the effectiveness of the propulsion work. Assume that each drive branch of the mechanism is 50mm at the shortest time, 100mm at the longest time, R=73.7mm, r=50mm, h=70mm; thus obtaining a three-dimensional map of the reachable working space under the constraint of the branch, as shown in Figure 9.

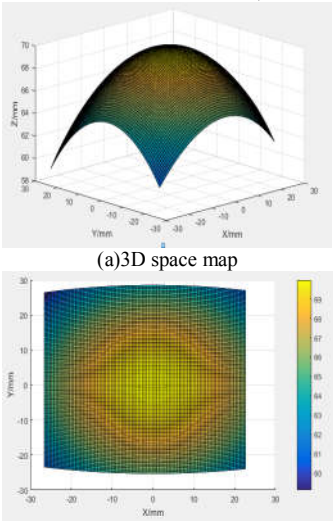

(a)3D space map

(b)Top view contour map

Fig. 9 The origin of the moving platform reaches the working space

Because the theoretical universal value of the angle of rotation along the two degrees of freedom of deflection is less than 90° (from the initial state of the mechanism), it does not affect the reachable workspace. Moreover, due to the limitation of the length of the driving branch rod, the deflection angles of the universal joints on the fixed platform in both directions must not reach 90°, so the size of the working space is still limited by the length of the branch rod. For the R pair of the UPR branch, the allowable angle of rotation is relatively large, and due to the limitation of the length of the branch rod, its corner will never reach its maximum and minimum limits, so the limitation of the corner to the working space can be ignored. For the universal joint of the UPU branch connected to the moving platform, the rotation angle δ_2 (shown in Fig 10) when the Y-axis rotates is large, and is limited by the length of the branch, so the corner does not work on the working space. It has an effect; when it rotates around the X axis, the size of the rotation angle δ_1 is limited. For this cross universal joint, the δ_1 at this time will not be greater than 15°, but due to the cooperation of the U pair below the branch, Within the limits of the length of the br`anch, this corner does not limit the working space. Because the UPR-UPU-UR mechanism has fewer parallel bars, there is no interference between the bars, and it does not affect the size of the workspace.

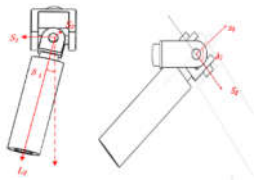

Fig. 10 Schematic diagram of the δ_i angle of the UPU branch

When considering the singular configuration, the initial conditions set are brought into equation (43), which can be obtained by matlab: α= 1.3970, β= 0.9505, both of which are larger than the range of the rod length limit, so the singular configuration can be ignored. influences.

$$\begin{cases} \alpha = \arctan(h/\sqrt{r^2+h^2}) \\ \beta = \arctan(h/r) \end{cases} \tag{43}$$

VI. CONCLUSION

In this paper, UPR-UPU-UR less-degree-of-freedom parallel vector propulsion mechanism is designed. According to the mechanism and its motion characteristics, a suitable coordinate system is established. After that, the kinematics analysis was carried out by analytical method, and the position inverse solution and the velocity and acceleration equations of the mechanism were obtained. The velocity inverse Jacobi matrix is derived by deriving the position inverse solution equation, and the singular configuration of the mechanism is analyzed by using Jacobian. The reachable workspace of the mechanism is also solved, and the motion performance of the mechanism is verified. Finally, using Matlab to simulate the equation of motion, the solvability of the equation is verified. Through the above research, the theoretical basis for subsequent control and gait planning analysis is laid.

REFERENCES

[1] S. Liu, “Dynamics of parallel robots with less degrees of freedom,” Science Press, 2015.11.

[2] X. Kong, Y. Jin, “Type Synthesis of 3-DOF multi-mode translational/spherical parallel mechanisms with lockable joints,” Mechanism & Machine Theory, vol. 25,pp. 323-333,2015.

[3] C. Chariot, O. Verlinden, “CPG tuning using sensory feedback for walking applications,”Proceedings of the ECCOMAS Thematic Conference on Multibody Dynamic, pp. 721-730, 2013.

[4] K. Vladislay, “Design modeling and characterization of a miniature robotics fish for research and education in biomimetic and hioinsniration,”IEEE/ASME Transactions on Mechatronics, vol. 18, no. 2,pp. 471-483, 2013.

[5] K. Xu, J. Zheng, X. Ding , “Structural Design and Motion Mode Analysis of Six-Wheel Leg Robot,”Journal of Beijing University of Aeronautics and Astronautics,vol. 42,no. 1,pp. 59-71. ,2016.

[6] B. Siciiano,L. Shavico, L Villani, et al. “Robotics Modeling, Planning and Control,” Xi'an Jiaotong University Press,pp. 177-218,2015.

[7] B. Wang, X. Nie, S. Han, “Design space and dexterity analysis of a planar two-degree-of-freedom parallel robot,”Journal of Mechanical Transmission, vol. 39,no. 4,pp. 37-40. 2015.

[8] X. Chen,F. Xie,X. LIU, et al, “A comparison study on motion/force transmissibility of two typical 3-DOF parallel manipulators:The sprint Z3 and A3 tool heads,”International Journal of Advanced Robotic Systems,vol. 11,no. 1,pp. 1-10 ,2014.

[9] X. Zhu, Y. Song, C. Sun,et al. “Structural characteristics and kinematics analysis of 2RRUR-2RSS parallel mechanism,”Journal of Agricultural Machinery, vol. 47,no. 12,pp. 408-415,2016.

[10] L. Feng,W. Zhang,Z. Gong,et al, “Research progress and current status of Delt series parallel robots,”Robotics, vol. 36,no. 3,pp. 375-384, 2014.